MINIREVIEW

Boron-Nitrogen Lewis Pairs in the Assembly of Supramolecular Macrocycles, Molecular Cages, Polymers, and 3D-Materials

Beijia Chen[a] and Frieder Jäkle*[a]

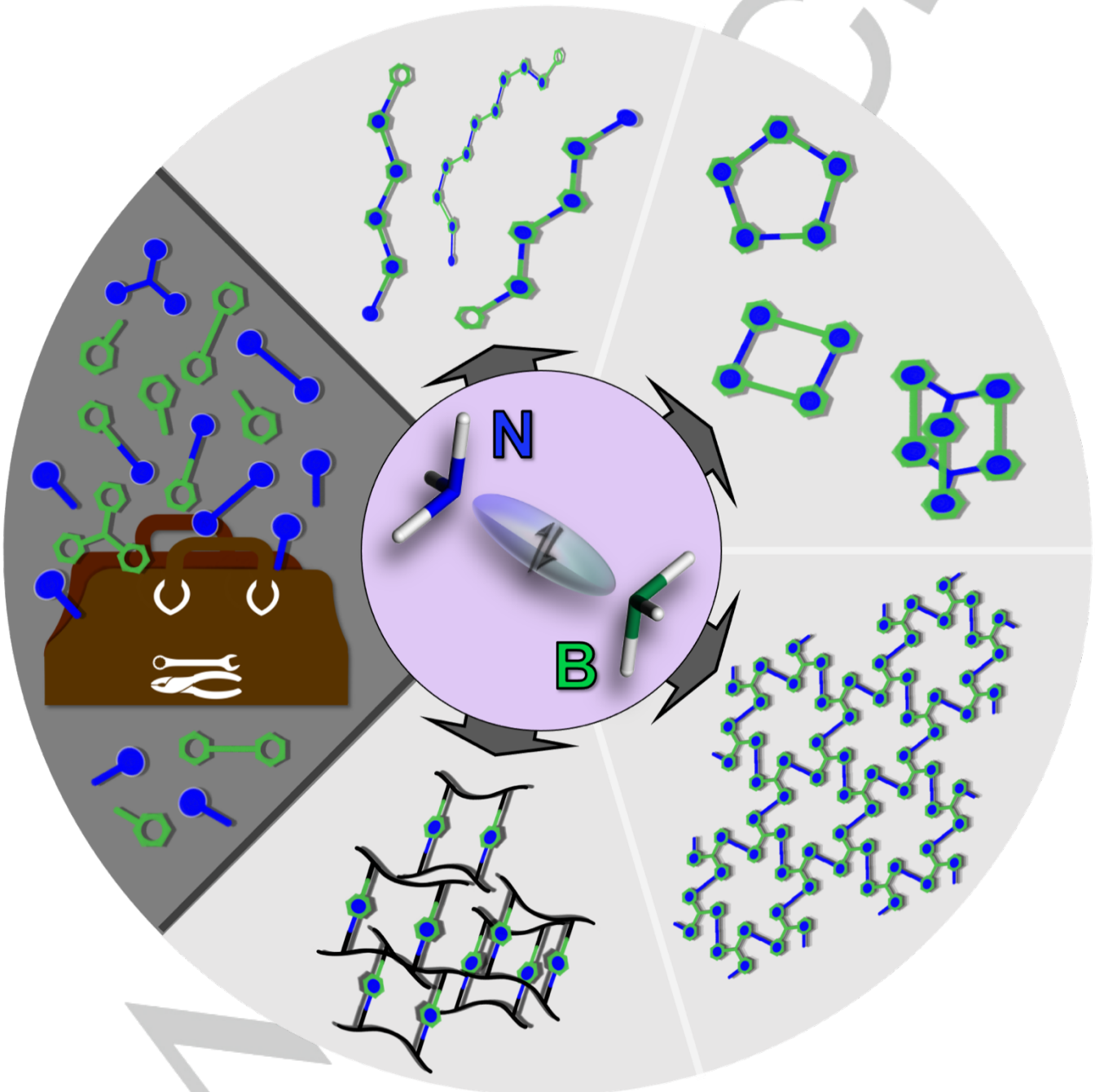

[a] B. Chen, Prof. Dr. F. Jäkle
Department of Chemistry
Rutgers University-Newark
73 Warren Street, Newark, NJ 07102, USA
E-mail: fjaekle@newark.rutgers.edu

Abstract: Covering an exceptionally wide range of bond strengths, the dynamic nature and facile tunability of dative B-N bonds is highly attractive when it comes to the assembly of supramolecular polymers and materials. This review offers an overview of advances in the development of functional materials where Lewis pairs (LPs) play a key role in their assembly and critically influence their properties. Specifically, we describe the reversible assembly of linear polymers with interesting optical, electronic and catalytic properties, discrete macrocycles and molecular cages that take up diverse guest molecules and undergo structural changes triggered by external stimuli, covalent organic frameworks (COFs) with intriguing interlocked structures that can embed and separate gases such as CO_2 and acetylene, and soft polymer networks that serve as recyclable, self-healing, and responsive thermosets, gels and elastomeric materials.

1. Introduction

The conceptualization of Lewis acids (LAs) and Lewis bases (LBs), and their interaction to form Lewis pair (LP) adducts, dates back to the seminal work by Gilbert N. Lewis in 1923.[1] Lewis' classification of LAs as electron pair acceptors and LBs as electron pair donors is still widely applied nowadays. In general, the interaction between a LA and a LB to form a LP constitutes an equilibrium reaction, and the energetics of that equilibrium depend on the nature of the constituting Lewis partners as well as external factors such as the temperature and concentration of the reagents (Figure 1). It was Herbert C. Brown and coworkers who in 1942 first described the impact that steric and electronic factors have on the energetics of adduct formation between boranes and amines.[2] Those studies not only set the stage for the use of such 'classical' LPs in supramolecular materials but also for what has since been classified as 'frustrated' Lewis pairs (FLPs). In FLPs, strong but sterically hindered LAs and LBs are prohibited from interacting directly (or do so only very weakly) but in concert effectively activate other small molecules. The FLP concept has been coined by Stephan and coworkers in 2006 to describe B/P LPs that activate dihydrogen,[3] and has since been expanded to virtually all parts of the periodic table.[4] FLPs nowadays play a prominent role in small molecule activation and catalysis.

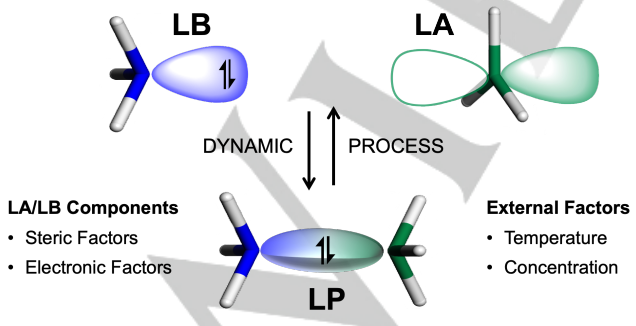

Figure 1. Schematic illustration of the dynamic equilibrium between a Lewis acid (LA) and a Lewis base (LBs) to form a Lewis Pair (LP).

As archetypical LPs, amine-borane adducts have been investigated extensively since Brown's early studies.[5] In the field of supramolecular chemistry, they play key roles in molecular recognition.[6] Beyond the formation of simple 1:1 LP adducts, systems where multiple LA sites interact with a Lewis basic substrate have attracted particular attention. In an early example, Katz and coworkers demonstrated that bifunctional boranes are capable of capturing hydrides in a bidentate fashion, acting as a 'hydride sponge' (**1**, Figure 2).[7] More recent work showed that multiatomic N-containing Lewis bases such as a azide, pyrazolide, hydrazine, pyridazine, pyrimidine or bipyridine can be captured effectively with tailor-made borane receptors through multiple B-N interactions (e.g., **2**, **3**).[8] The capture of substrates via B-N LP formation has also been coupled to small molecule activation processes.[9] For example, Wegner and coworkers employed diboraanthracenes as bifunctional catalysts in inverse-demand Diels-Alder reactions of 1,2-diazenes.[9f,g] Moreover, the capture of hydrazine by a bidentate borane in the coordination sphere of the transition metal complex **4** led to metal-mediated N-N bond cleavage.[9b] Even cooperative N_2 activation has been achieved with a diboraanthracene-samarocene pair.[9d] B-N LP formation has also been exploited to position photoactive molecules in close proximity to one another in a way that allows for topochemical [2+2] olefin photodimerization to occur rapidly (e.g., **5**) [10] or to trigger visible light-fueled photomechanical processes.[11] Finally, B-N LP formation has been exploited to modulate the electronic structure and photophysical properties of π-conjugated organic materials. For instance, the band gap of π-conjugated polymers containing N-heterocyclic building blocks can be effectively altered via B-N LP formation.[12] In addition, recent studies show that interesting photophysical properties, such as tunable fluorescence, long-lived phosphorescence, or piezochromic behavior can be achieved by utilizing B-N LP interactions in the design of molecular crystals (e.g., **6**).[13]

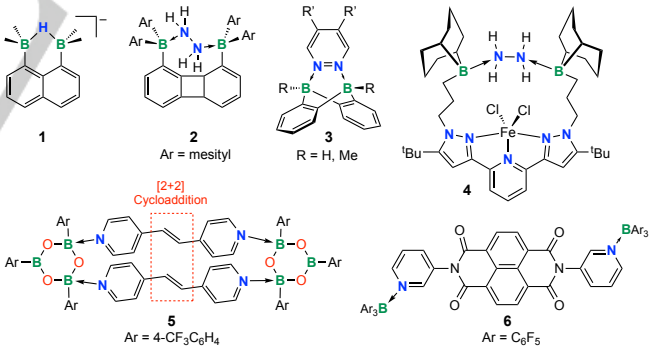

Figure 2. Examples of molecular systems with multiple B-N LP interactions.

In this review we will focus on recent advances in the use of multiple dynamic B-N LPs to assemble macromolecules, including macrocycles, molecular cages, linear polymers, and 3-D network materials. Polymeric structures based on B-N LP formation were postulated by Niedenzu and coworkers for (1-imidazolyl)diorganylboranes as early as 1975,[14] and discrete macrocyclic species were first isolated and structurally characterized by single crystal X-ray diffraction in 1991.[15] Since these initial efforts much progress has been made in the development of supramolecular polymeric materials using boronic acids and boronate esters,[16] boroxines[17], or triorganoboranes in combination with amines. In here, we will only consider systems

where the B-N LP formation is the sole motif for linking together molecular building blocks. Materials that are assembled using, for example, N,O- or N,C-chelate ligands are not discussed but are included in some recent reviews to which the interested reader is referred to.[18] We will also not elaborate on aminoborane polymers with alternating B and N atoms in the main chain, which may be considered as polymeric forms of iminoboranes that are assembled through B-N LP bonding. The reader is referred to an excellent review by Manners and coworkers on this topic.[5]

Beijia Chen received her Bachelor's degree in Polymer Material and Engineering at Harbin Institute of Technology (Harbin, China) in 2018 and Master's degree in Polymer Composite Science and Engineering at the University of Sheffield (Sheffield, UK) in 2019. Currently she is working on her PhD at Rutgers University Newark under the supervision of Prof. Frieder Jäkle. Her research interests focus on the synthesis of functional polymeric materials.

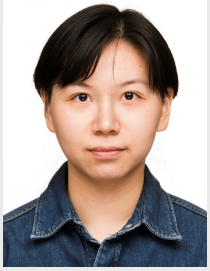

Frieder Jäkle is a Distinguished Professor in the Department of Chemistry at the Newark campus of Rutgers University. He received his Diploma in 1994 and Ph.D. in 1997 from TU München, Germany, under the direction of Prof. Wagner. After a postdoctoral stint with Prof. Manners at the University of Toronto he joined Rutgers University in 2000. His research interests revolve around main group chemistry as applied to materials and catalysis, encompassing projects on organoborane Lewis acids, conjugated hybrid materials, luminescent materials for optoelectronic and sensory applications, and stimuli-responsive and supramolecular polymers.

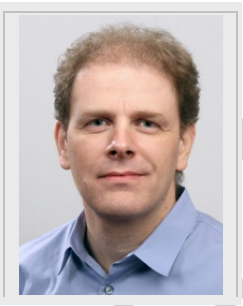

2. Supramolecular Main Chain Polymers

Conventionally, introduction of boron atoms into the backbone of a polymeric material most commonly involves hydroboration, organometallic condensation or coupling reactions of boron-containing monomers, which produce polymer chains with only strong covalent bonds.[19] In pursuit of dynamic polymers that can be assembled and disassembled upon demand by application of a stimulus,[20] several research groups have set out to assemble linear polymers from complementary bifunctional LA and LB monomers by reversible B-N LP formation. Boronic acids and their anhydrides, boronic esters, and triorganoborane have all been used as the LA component and combined with ditopic heteroaromatic or (rigid) aliphatic amines. Bifunctional A-B type building blocks containing both LA and LB sites have also been developed. Selected examples of polymeric materials that were assembled from 'classical' LPs are presented, as well as a very recent example of 1-D polymer stacks derived from sterically hindered FLPs.

2.1. Polymers Derived from 'Classical' Lewis Pairs

The reversible formation of boronate esters through dynamic covalent bond formation of boronic acids with diols has been widely explored in materials and biomedical applications.[16, 21] Studies by Severin, Höpfl, Salazar-Mendoza, and other groups showed that dative B-N interactions can be used in parallel with boronate ester condensation to generate novel polymer architectures by three-component reactions. In one example, Severin and coworkers generated LP polymers using ditopic N-donor ligands as linkers between boronate moieties (**7**, Figure 3a). Deeply colored purple polymers precipitated from a hot mixture of 1,2-bis(4-pyridyl)ethylene (or 4,4'-bipyridine), two equivalents of a phenylboronic acid derivative, and one equivalent of 1,2,4,5-tetrahydroxybenzene in benzene.[22] The structure of the linear polymer with Ar = 3,5-dimethylphenyl, X = none was verified by crystallographic analysis (Figure 3a, inset). The relatively long B-N bonds (1.702(5) Å) compared with those observed for typical small molecule B-N adducts suggested a weak interaction between the bis(pyridyl) bridges and the boronate esters. The strong color of the polymers in the solid state was attributed to intramolecular charge transfer (ICT) along the polymer backbone based on DFT calculations. However, upon dissolution in hot chloroform the color changed to light yellow, which suggested that the dative B-N bonds were not retained in solution. In a similar manner, bifunctional A-B type monomers were utilized by Höpfl, Salazar-Mendoza and coworkers. Reaction of 3-pyridyl or 5-isoquinolinylboronic acid with 1,2-ethanediol or 1,3-propanediol under Dean-Stark conditions yielded the respective boronate esters which assembled into 1D polymers with B-N distances ranging from 1.669(3) Å to 1.684(3) Å) (**8**, Figure 3b).[23] It is important to note that linear polymer assembly competes with formation of macrocycles (*vide infra*), and the nature of the isolated product appeared to be determined to a large extent by intermolecular interactions in the solid state. Again, all these B-N LP polymers dissociated in solution. Although none of these polymers were stable in solution, the reversible formation of the polymer backbone highlighted the potential of boronic acids and esters as building blocks for the generation of supramolecular polymers with interesting new structures and properties.

Efforts have been made to achieve supramolecular polymers that retain their self-assembled structure in solution by increasing the B-N interaction strength. Severin and coworkers demonstrated that when spatially separating the pyridine and boronate ester groups in A-B type bifunctional monomers it is possible to increase the strength of the dative B-N bonds in substantially (**9,** Figure 3b). The borane LA strength was enhanced by substitution of the aryl groups with electron-withdrawing fluorine and the pyridine LB strength by substitution with electron-donating amino groups.[24] Association constants of over 10^6 M^{-1} and appreciable viscosities in solution were indicative of high molecular weight materials that retained the polymeric structure in solution. Similarly, use of more Lewis basic imidazolyl as opposed to pyridyl donors in A_2-B_2 monomer systems resulted in high molecular weight polymers (**10**, Figure 3c).[25] By screening different combinations of 1,4-phenylenediboronic catecholate esters with bisimidazolyl ligands having different spacer groups, polymers that formed strong gels with sol-gel transition temperatures of over 100 °C were obtained. Scanning electron microscope (SEM) was used to examine the network morphology of the polymer gels after freeze drying (Figure 3c, inset). A fibrillar network was observed, and the diameter of the fibers was estimated to be less than 100 nm on average. A photo-responsive

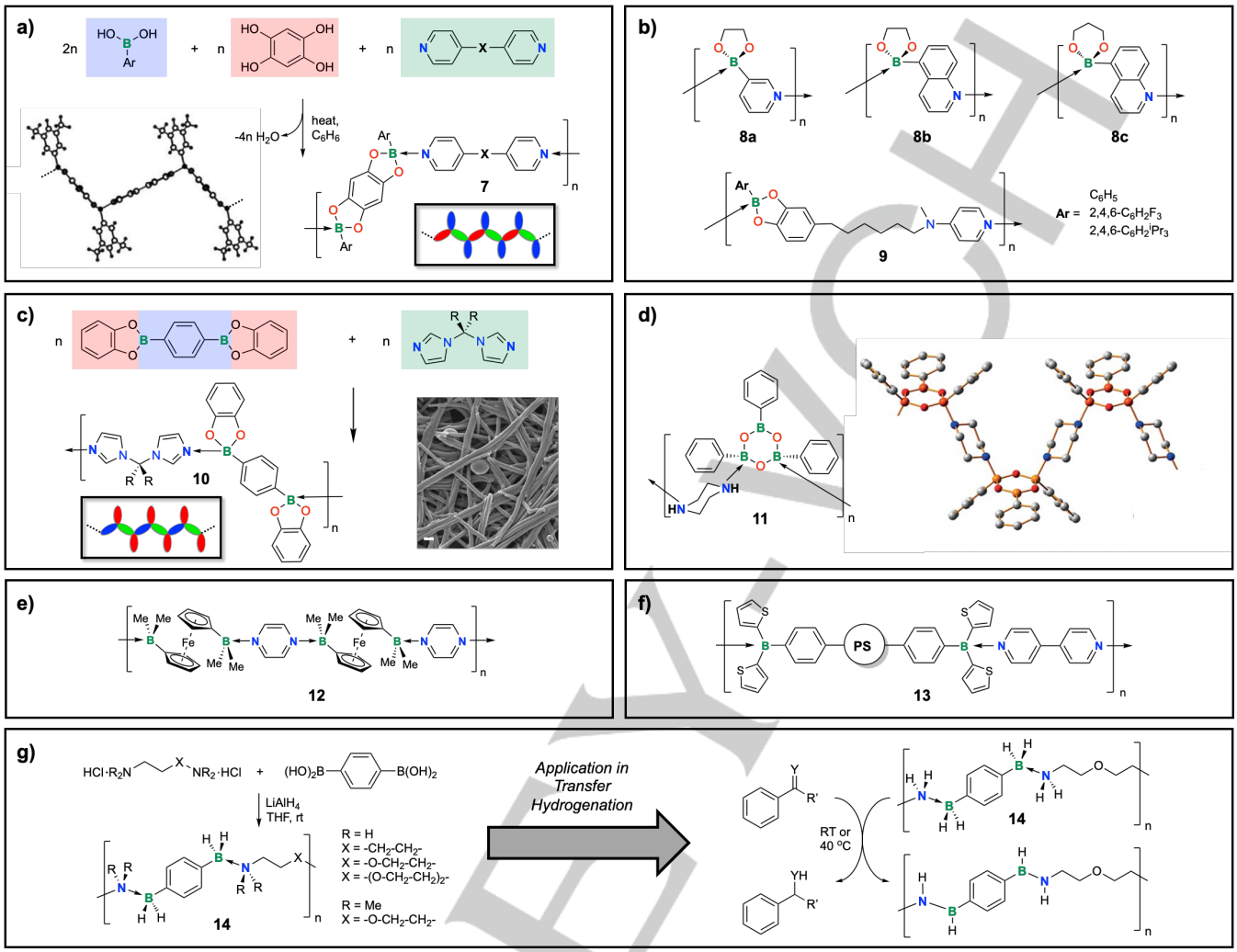

Figure 3. Examples of linear polymers based on dynamic B-N LP formation in the main chain. a) Polymerization of bis(boronates) generated *in-situ* from boronic acids and tetrahydroxybenzene with bis(pyridines); Ar = 4-ethylphenyl, 3,5-dimethylphenyl, 4-*t*-butylphenyl; X = none, *trans*-ethylene; insets: schematic illustration of polymer structure and X-ray structure for polymer with Ar = 3,5-dimethylphenyl and X = none. b) Examples of polymers derived from A-B type bifunctional monomers. c) Polymerization of 1,4-bis(benzodioxaborolyl)benzene and bis(imidazolyl)alkanes (R = H, Me) with gel formation, insets: schematic illustration of polymer structure and SEM image of xerogel obtained by freeze-drying the polymer gel (R = H, scale bar: 200 nm). d) Supramolecular polymer derived from boroxine formation in the presence of a diamine; inset: depiction of X-ray structure (C grey, O red, B orange). e) Redox-active ferrocene-containing dynamic polymer derived from diborylated ferrocene and pyrazine. f) Supramolecular polystyrene derived from borane end-functionalized low molecular weight polystyrene (PS) and 4,4'-bipyridine. g) Polymers derived from aliphatic diamines and phenylene diboronic acid and their use in transfer hydrogenation reactions (Y = H, R' = NMe, N*t*Bu, NPh, NSO_2Ph or Y = O, R' = Me). Images adapted with permission from refs. 22 (a), 25 (c), and 26 (d).

gel was also generated by using a diboronate ester with an azobenzene bridge. Collectively, these results represented important first steps towards the development of functional soft materials based on dative B-N bonds.

Boroxines, the trimeric anhydrides of boronic acids,[17] have also proven highly useful as building blocks for supramolecular materials. Usually only one or two of the three boron atoms in boroxines participate in B-N bond formation as binding to the third boron tends to be thermodynamically rather unfavorable. This provides an opportunity to use boroxines as ditopic building blocks in combination with ditopic amines for the formation of 1D-supramolecular polymers. In one example, Höpfl, Salazar-Mendoza and coworkers reacted phenylboroxine, generated *in-situ* from phenylboronic acid, with 1,4-diazacyclohexane (piperazine) in dimethylformamide under reflux.[26] The B-N bond lengths in the resulting coordination polymer (**11**, Figure 3d) of 1.681(4) and 1.688(4) Å are relatively long suggesting that the polymer would not retain its structure in solution. Further studies by Jancik and coworkers indicated that the product structure strongly depends on the nature and size of the crystallization solvent. Larger donor solvents such as pentanone favored formation of molecular 2:1 adducts but chlorinated solvents (chloroform or dichloromethane) resulted in 2:3 adducts of boroxine:piperazine in which one of the piperazines adopted a bridging position.[27] Most recently, Van Hecke and coworkers reported the mechanochemical synthesis of polymers comprising phenylboroxines and 1,4-diazabicyclo[2.2.2]octane (DABCO).[28] They demonstrated that the substituents on the phenyl groups

impact the product distribution where electron-withdrawing halides favor polymeric over molecular structures because of the enhanced Lewis acid strength.

Triorganoboranes can be expected to offer access to stronger adducts than boronic esters or boroxines due to the increased Lewis acidity at boron in the absence of B-O π-bonding interactions. An interesting example is the generation of metal-containing macromolecules via B-N coordination. Pursuing novel synthetic routes to poly(ferrocene)s, Wagner and coworkers explored the formation of polymers with a dynamic backbone that consists of diborylated ferrocenes linked by 4,4'-bipyridine or pyrazine (**12**, Figure 3e).[29],[30] The polymeric nature in the solid state (but not in solution) was demonstrated by infrared spectroscopy and single crystal X-ray analysis. The polymer containing pyrazine was green and that containing 4,4'-bipyridine was deep purple colored due to ICT from the electron-rich ferrocene to the electron-deficient pyrazine/bipyridine units. Electrochemical analyses revealed electronic delocalization along the polymer backbone promoted by the N-heterocycle π-systems. These studies offer an elegant approach to supramolecular materials that combine the advantageous redox characteristics of poly(ferrocene)s with the electron-accepting properties of the bipyridyl and pyrazine units.

Multiply charged supramolecular polymers were accessed by B-N LP formation between diborylated imidazolium-based ionic liquids and pyrazine or 1,4-diazabicyclo[2.2.2]octane.[31] Matsumi and coworkers reported that these polymers were soluble in highly polar solvents such as methanol, showing ^{11}B NMR signals in the expected region of tetracoordinate boron. Lithium ion conductivities of up to 8.8 $\times$ 10^{-6} S cm^{-1} at 51 ºC were measured in the presence of equimolar amounts of lithium triflimide, $LiNTf_2$.

Our group showed that borane-end-functionalized polymers could be assembled into further elongated polymeric structures by B-N bond formation.[32] Treatment of ditelechelic polystyrene Th_2B-PS-BTh_2 (Th = 2-thienyl) with 4,4′-bipyridine in CH_2Cl_2 produced extended polymer chains [Th_2B-PS-BTh_2·bipy]$_n$ through B-N LP formation (**13**, Figure 3f). The product was easily isolated by precipitating the reaction mixture into hexanes. ^{1}H NMR integration showed the presence of one 4,4′-bipyridine molecule per polystyrene chain and ^{11}B NMR spectroscopy showed a single peak at 0 ppm consistent with pyridine-bound tetracoordinated boron atoms. DSC studies revealed a glass transition temperature of 105 °C for **13**, which was significantly higher than that of the low molecular weight starting material Th_2B-PS-BTh_2 (88 °C), further confirming assembly into polymer chains of considerably higher molecular weight. These results also provided inspiration for using borane-functionalized polymers capable of B-N bond formation to create more complex copolymer network architectures (*vide infra*).

The above examples were focused mostly on the use of bipyridines or pyrazines with bis-borane linkers, but other Lewis bases can also be used in the assembly of main chain polymers through LP formation. Recently, ammonia borane (NH_3·BH_3) has become an essential area of research for dihydrogen-storage materials.[33] To overcome some of the shortcomings of ammonia borane, such as poor processability and recyclability, Lacôte's group was fascinated by the idea of using polymeric amine-boranes to achieve dehydrogenation.[34] In earlier works, Manners and coworkers had demonstrated that phosphine-borane and amine-borane adducts can be utilized as precursors to polymers that contain alternating B/P or B/N in the main chain via dehydrocoupling polymerization.[5, 35] Lacôte and coworkers developed a new approach to polyboramine polymers by treatment of a mixture of *para*-phenylene-bis(boronic acid) and bis(ammonium) salts with $LiAlH_4$ in THF (Figure 3g, left). Polymers **14** precipitated from the reaction mixture, and number-averaged molecular weights of over 10^5 g/mol were measured by size exclusion chromatography (SEC). Temperature-programmed desorption (TPD) measurements showed that these polyboramines can liberate H_2 below 100 °C. Although, the dehydrogenation appeared to increase the molar mass of the polymers to a certain extent, possibly due to intermolecular interactions, they still maintained solubility in polar solvents indicating good processability of the bulk material. One of the polymers was used to hydrogenate imines, aldehydes, and ketones under mild conditions (Figure 3g, right), performing better than the respective molecular analogues. Analysis of the polymer by NMR spectroscopy after reduction indicated that only the first equivalent of H_2 was transferred to the substrates. It was hypothesized that the polymer chain architecture might have a specific effect on the thermal dehydrogenation, hence theoretical modeling was carried out to examine the reaction pathways. A plausible dehydrogenation pathway was postulated that involves the cleavage of a B-N bond with formation of a key intermediate that is more favorable for the polymer chains than the molecular species because of entropic effects. This work demonstrated the utility of polymers incorporating B-N LPs in the main chain for dihydrogen-storage while also highlighting the fascinating prospects for catalysis applications.

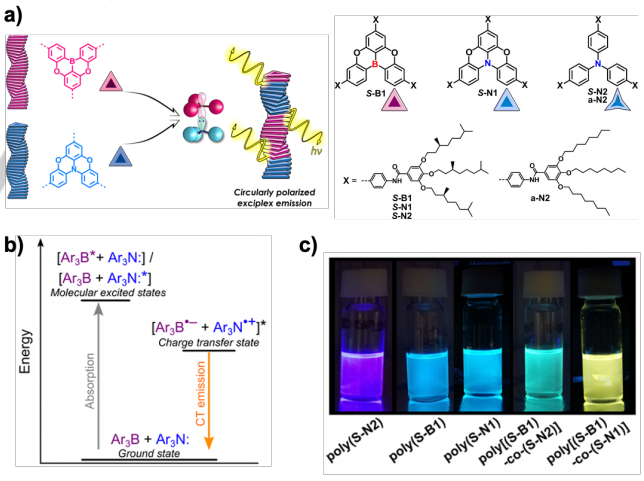

Figure 4. Assembly of 'frustrated' B-N LPs into 1D supramolecular stacks. a) Chemical structures of B and N monomers and schematic illustration of their assembly into homopolymers and copolymers with circularly polarized exciplex emission. b) Schematic representation of the mechanism of CT emission in the copolymers. c) Photographs of the emission of supramolecular homopolymer and copolymer solutions in decalin at 20 ºC under a long-wavelength UV lamp. Adapted with permission from ref. 36.

2.2. Polymers Derived from 'Frustrated' Lewis Pairs

Besides the polymerization of 'classical' B-N LPs it is also possible to construct 1D supramolecular assemblies from 'frustrated' LPs (FLPs). Research by Yamaguchi, Meijier and coworkers showed successful incorporation of triphenylboranes

and triphenylamines as frustrated B-N LPs into linear supramolecular copolymer stacks (Figure 4a).[36] For the design of the B building block they chose an O-bridged triphenylborane (**S-B1**) because the relatively electron-rich environment and structural rigidity impart high stability to the boron core. Two types of N building blocks (**S-N1**, **S-N2**) were synthesized to accommodate H-bonding supramolecular motifs and induce chirality to the aggregates. First, individual assemblies of the B and N units were studied by circular dichroism (CD) showing preferred helicity. Then, supramolecular copolymerization reactions were performed by heating a mixture of poly(**S-B1**) and an equimolar amount of either poly(**S-N1**) or poly(**S-N2**) to reach the molecularly dissolved state, followed by slow cooling to form aggregates under thermodynamic control. The formation of random block-like copolymers was deduced using a combination of photoluminescence studies and optical spectroscopic techniques. It was hypothesized that the formation of FLPs between the π-conjugated N donor and B acceptor could result in charge-transfer (CT) processes in the ground and/or excited states of the resultant copolymer assemblies (Figure 4b). The formation of new aggregated states was visible to the naked eye as changes in emission color were readily observed for poly[(**S-B1**)-*co*-(**S-N2**) and poly[(**S-B1**)-*co*-(**S-N1**)] (Figure 4c). Lifetime measurements confirmed the formation of B-N exciplexes as the emission exhibited two decay components. The longer photoluminescence decay component was attributed to forbidden transitions from charge transfer (CT) excited states. Further evidence came from emission lifetime measurements in oxygen-free solvents which indicated the presence of a long-lived triplet excited state, similar to ones previously reported in B-N OLED materials. Polarized optical microscopy and X-ray scattering indicated the formation of a hexagonally packed cylindrical phase with a domain spacing of 3.4 nm for the copolymers. These pioneering studies into converting FLPs into 1D supramolecular copolymers provided an interesting solution to define the microstructure of a copolymer. Furthermore, the circularly polarized CT emission of the chiral assemblies could have potential applications in supramolecular optoelectronics utilizing the electronic communication between FLP donors and acceptors.

3. Supramolecular Macrocycles and Cages

Thus far, we have focused on how monomeric precursors can be linked together into dynamic 1D linear chains by B-N LP chemistry. Much research has also been devoted to the assembly of 2D macrocycles and finite 3D cage structures by varying the number and spatial arrangement of the functional groups within the molecular building blocks.[37] This is attractive because, contrary to traditional approaches to covalently linked systems, well-defined supramolecules can be obtained in a reversible manner, with the dynamic bonding enabling interconversion between discrete structures.

3.1. Assembly of Macrocycles via B-N Lewis Pairs

The incorporation of boron into macrocycles has long inspired researchers due to the potential for unusual optical and electronic properties, as well as opportunities for self-assembly and host guest chemistries as a result of their unique shape.[38] Early efforts to generate macrocyclic species through B-N LP formation date back to 1991 when Niedenzu reported the crystal structures of cyclic tetramers of (triazolyl)dimethylborane **(15)** and related (benzotriazolyl)dimethylborane obtained by reaction of Me_2BBr with the respective N-silylated triazoles (Figure 5).[15] B-N bond formation at the N1 and N3 nitrogens of triazole led to assembly into tetrameric structures, contrasting the formation of dimeric pyrazaboles (**16**) upon B-N bond formation at neighboring N atoms in pyrazolylboranes. Later, Siebert and coworkers showed that discrete tetrameric (or pentameric) macrocycles (**17**) are generated in a similar manner from imidazolylboranes when small substituents are used on boron (R = H, Me).[39]

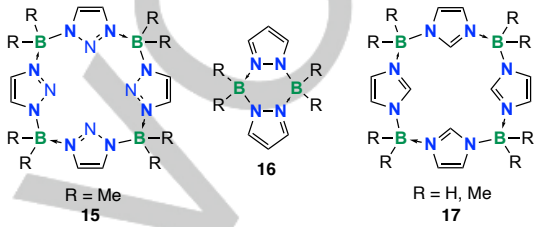

Figure 5. Early examples of macrocycles obtained via B-N LP formation.

Since then, the assembly of many other LA-LB pairs into macrocyclic architectures has been explored. In the previous section, we presented works by Severin, Höpfl and others that showed that dative B-N interactions can be combined with boronate ester condensation to obtain linear polymers. Severin and coworkers also demonstrated that condensation of aryl- and alkylboronic acids with 3,4-dihydroxypyridines affords pentameric macrocycles through dative B-N bonds between complementary LA and LB sites (**18**, Figure 6a).[40] Crystal structures showed the incorporation of weakly bound benzene solvent molecules. They also revealed that, while all five boron atoms in the pentamers represent stereogenic centers, the cyclic structures were highly symmetric and all boron atoms had the same configuration. Short B-N bond lengths (1.600(16)-1.608(9) Å) suggested strong interactions and high stability, which formed the basis for their use as building blocks of dendritic nanostructures such as **19** (Figure 6a).[40] To this end, arylboronic acids with aldehyde functionalities were used which, after assembly of the macrocycles, allowed for attachment of amine-functionalized dendrons via imine bond formation. These results highlight the possibility of post-synthesis functionalization of macrocycles by attaching suitable pendent groups to the B-N coordinated core.

Much work has also been devoted to studies on macrocyclic species derived from pyridylboranes in which covalent B-C and dative B-N bonds alternate within the macrocyclic framework. In 1996, Sugihara, Takakura and coworkers demonstrated that 3-(diethylboryl)pyridine (**20**) forms a tetrameric macrocycle via intermolecular B-N LP formation. The tetrameric structure was confirmed by single crystal X-ray diffraction analysis and found to be retained in solution according to vapor pressure osmometry studies (Figure 6b).[41] Furthermore, scrambling experiments suggested that the macrocycle is stable in toluene up to 60 °C for extended periods of time but undergoes scrambling at 100 °C. In subsequent studies, Wakabayashi and coworkers explored the assembly of 3-(diethylborylalkynyl)pyridine (**21**) which preferentially adopted a trimeric structure in solution and the solid

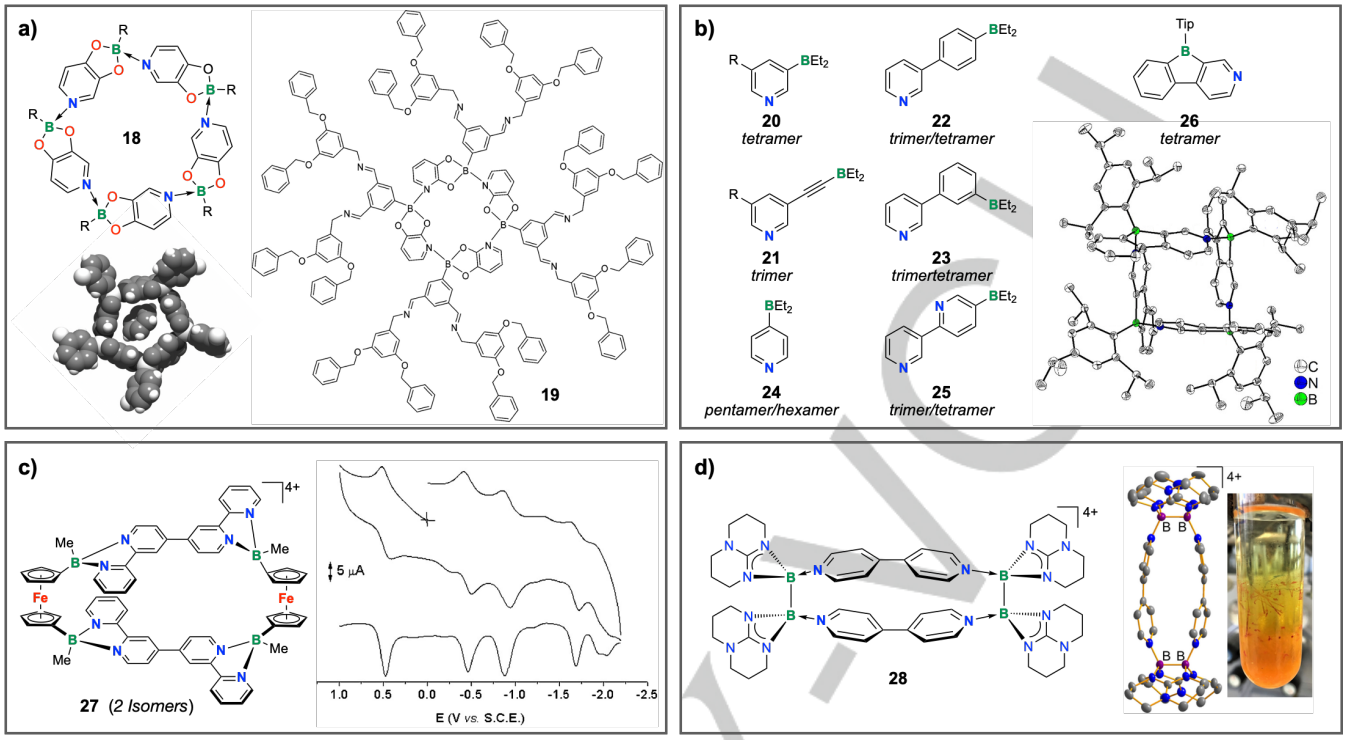

Figure 6. Examples of dynamic macrocycles based on B-N LP formation. a) Examples of pyridylboronate macrocycles **18** (R = *p*-C_6H_4Me, *p*-C_6H_4*t*Bu, *p*-C_6H_4F, *p*-C_6H_4CHO, *p*-$C_6H_4NH_2$, *n*-Bu), space-filling model of benzene inclusion complex for macrocycle **18** with R = *p*-C_6H_4F, and use as scaffold for dendrimer **8**. b) Examples of borylated pyridine derivatives **20**-**26** that form macrocycles (R = H, OCH_3, $OCH_2CH_2OCH_3$, Tip = 2,4,6-triisopropylphenyl) and plot of the X-ray crystal structure of the pyridyl-fused antiaromatic borole **26**. c) Ferrocene-containing boronium macrocycles **27** and illustration of cyclic and square wave voltammograms. d) Example of a diborane-containing macrocycle **28**, its X-ray crystal structure and photograph illustrating its bright orange color. Images adapted with permission from refs. 40 (a), 47 (b), 48 (c), and 49 (d).

state and underwent scrambling at a relatively lower temperature of 80 °C in toluene.[42] They also found that phenylene-bridged 3-[3'-(diethylboryl)phenyl]pyridine (**22**) and 3-[4'-(diethylboryl)-phenyl]pyridine (**23**) form dynamic mixtures of trimeric and tetrameric macrocycles in solution even at room temperature.[43] Larger cyclic pentamers and hexamers were detected in the assembly of (4-diethylboryl)pyridine (**24**), in which the boryl group and pyridyl donor are positioned at a 180° angle.[44]

Importantly, the dynamic equilibrium established in solution offers an opportunity to access differently sized macrocycles from one and the same molecular building block. By controlling the crystallization conditions, Wakabayashi and coworkers showed that judicious choice of solvent and temperature makes it possible to selectively crystallize a specific macrocycle of 3-[4′-(diethylboryl)phenyl]pyridine (**23**) or (4-diethylboryl)pyridine (**24**).[44-45] Solvent molecules such as benzene were incorporated into the crystal lattice, thereby shifting the equilibrium throughout the crystallization process. The re-equilibration upon dissolution of the crystals was studied for the pyridyl-bridged analog (5-diethylboryl)-2,3'-bipyridine (**25**) by means of flow-NMR experiments.[46] This technique allows one to monitor the equilibration process on time scales of less than 1 minute and in dependence on the nature of the solvent.

In a recent study, Marder and coworkers showed that the pyridyl-fused antiaromatic borole **26** forms a tetrameric macrocyclic species in solution and the solid state (Figure 6b, right).[47] The B-N bond distances (1.644(2)-1.655(2) Å) are comparable to those of sterically hindered dibenzoborole-pyridine adducts. However, in contrast to these molecular complexes that dissociate in solution at room temperature, the tetrameric structure of **26** persisted in C_6D_6 at 50 °C. The macrocycle showed an absorption maximum at 322 nm and an emission at 495 nm. Based on the short fluorescence lifetime of 6 ns the emission was postulated to arise from the tetracoordinate macrocycle itself rather than a photo-dissociated tricoordinate species. Collectively, these studies demonstrated that the size and dynamic exchange between macrocycles is critically influenced by steric and electronic effects, including the nature of the linker and attachment point of the Lewis acidic boryl groups, as well as the solvent and crystallization conditions.

It is also possible to construct metal-containing macrocycles via B-N LP interactions as demonstrated by Wagner's group. Two ferrocenylborane units were linked by 2,2:4,4:2,2-quaterpyridine to afford the macrocycle **27** (Figure 6c).[48] NMR data and GPC results confirmed the cyclic structure. Cyclic and differential pulse voltammetry data displayed a four-step reduction pattern, as well as a single ferrocene-centered oxidation, which was measured to consume 2 electrons. These results supported the proposed macrocyclic structure while also suggesting that any electronic communication remained confined within the quaterpyridine linker.

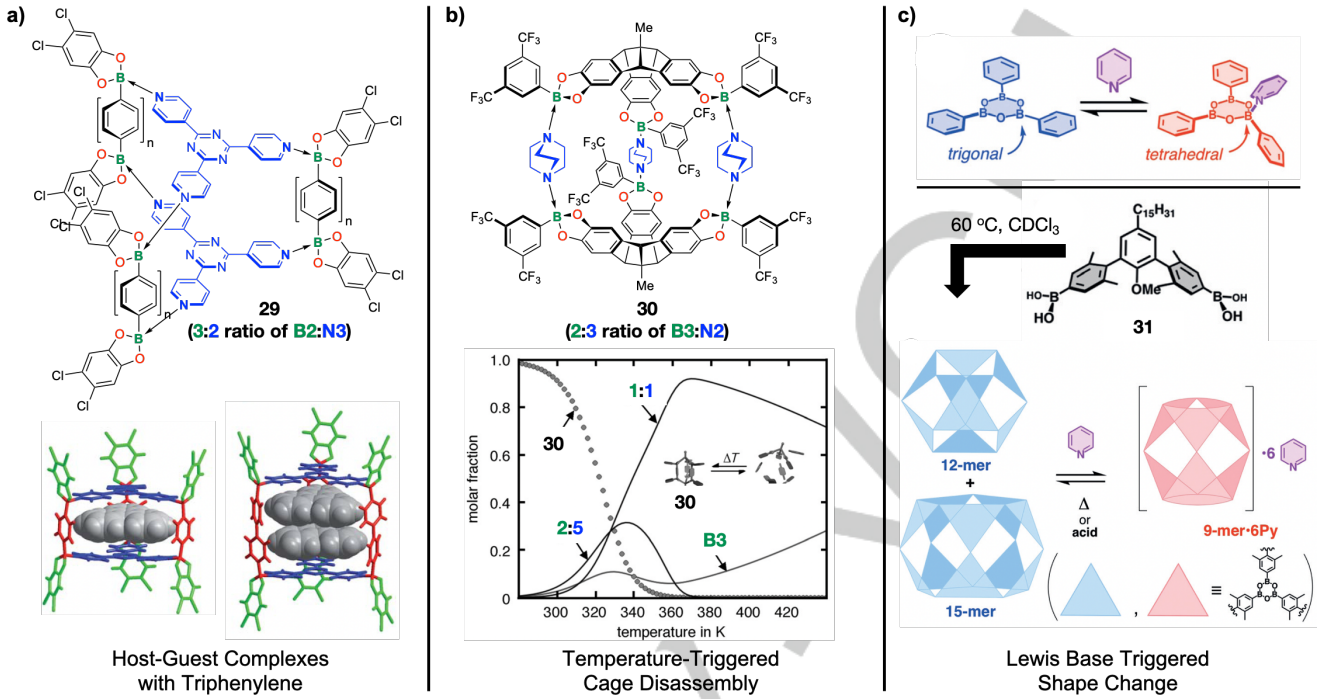

Figure 7. Examples of dynamic molecular cages based on B-N LP formation. a) Prismatic cage **29** derived from tritopic 2,4,6-tri(4-pyridyl)-1,3,5-triazine (**N3**) and a ditopic diboronate ester (**B2**), and illustration of inclusion complexes with triphenylene. b) Trigonal bipyramidal cage **30** derived from a tritopic borane (**B3**) and a ditopic amine (**N2**) and its temperature-dependent disassembly/reassembly. c) Pyridine-triggered dynamic transformation of boroxine-based cages derived from ditopic boronic acid **31**. Adapted with permission from refs. 51 (a), 52 (b), and 55 (c).

The fascinating redox properties of these macrocycles may inspire the development of applications in the field of electron sponges and anion recognition.

Himmel and coworkers assembled polycationic boronium macrocycles **28** from electron-rich diborane building blocks (Figure 6d).[49] With 4,4'-bipyridine or more extended bis(pyridine)s, cyclic dimers were generated preferentially. Cyclic tetramers were found in some cases as a minor component. Computational studies suggested the orange color of the products to be due to ICT from the electron-rich diborane moieties to the electron-deficient bis-pyridine linkers.[50]

3.2. Assembly of Molecular Cages via B-N Lewis Pairs

While the macrocyclic architectures discussed above were generated from complementary ditopic precursors, the assembly of 3D cage structures can be achieved by connecting appropriately shaped tritopic building blocks with ditopic linkers.[37] For example, Severin's group demonstrated that dative B-N bonds can be used in conjunction with boronate esters to construct prismatic cages such as **29** in multicomponent condensation reactions (Figure 7a).[51] 2,4,6-tri(4-pyridyl)-1,3,5-triazine (tpt, **N3**) was chosen as the tritopic building block and diboronate esters (**B2**) were used as ditopic linkers. Single crystals of the cages were obtained by slow cooling of a hot 1,2-dichlorobenzene solution and host-guest complexes co-crystallization with triphenylene or coronene (Figure 7a, bottom). Crystallography data showed that the planar aromatic guests were located centrally between the two tpt walls at typical π-stacking interaction distances of ca. 3.5 Å. A larger cavity volume was achieved by using longer biphenyl struts, allowing accommodation of two aromatic guests. Multiply charged cages of this type have recently been reported by Himmel and coworkers to form upon assembly of tpt with dicationic diborane moieties as linkers.[50] These cages are strongly colored and redox-responsive, offering potential opportunities for redox-triggered guest uptake and release. It will be interesting to see whether the use of dative B–N bonds can be extended to other types of cage structures and whether such host-guest systems could prove useful also in gas storage and related applications.

The opportunity to reversibly assemble and disassemble the cage structure by application of a stimulus is a particularly attractive feature of dynamic B-N LPs. Beuerle's group designed and synthesized a trigonal bipyramidal supramolecular cage **30** (Figure 7b) that exists as a discrete species in solution and studied the reversible cage opening/reassembly processes in detail.[52] The requisite trigonal trisboronate ester scaffold (**B3**) was obtained by reacting catechol-functionalized tribenzotriquinacene with bis(trifluoromethyl)phenylboronic acid. 1,4-Diazabicyclo[2.2.2]octane (**N2**) was then added as a rigid linear bifunctional LB to achieve supramolecular assembly. The assembly process was investigated by isothermal calorimetry (ITC), variable temperature (VT) and Diffusion Ordered Spectroscopy (DOSY). The results suggested that a single cage species was present at room temperature, but cage opening could be triggered by addition of acid or an increase in temperature. VT

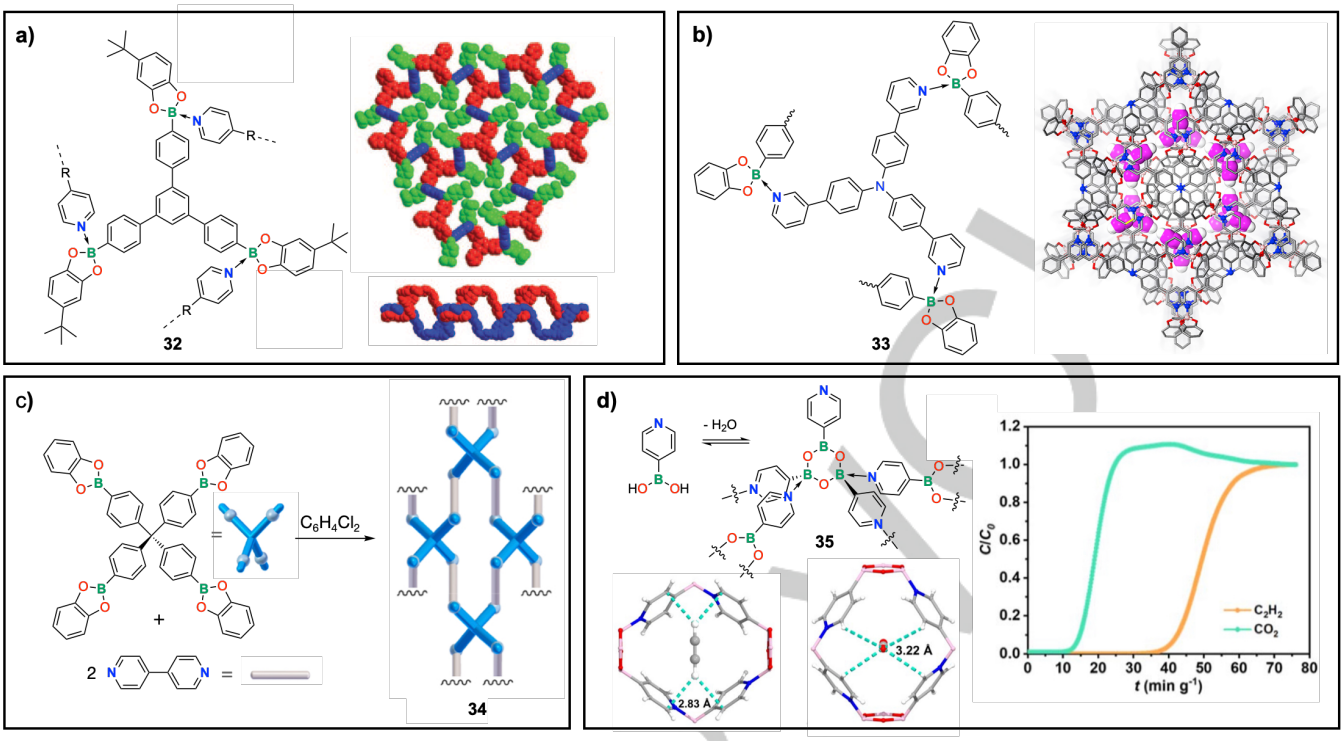

Figure 8. Examples of COFs based on B-N LP formation. a) COF **32** derived from trifunctional borane and bifunctional amine (R = none, vinylene); inset: space-filling view of the 2D network structure of **32** (R = vinylene, boronic acid in red, bis(pyridine) in blue, catechol in green) and illustration of how layers are interwoven (catechol groups removed for clarity). b) COF **33** derived from trifunctional amine and bifunctional borane; inset: packing diagram of **33**@C_2H_2 viewed along the *ab* plane. c) Formation of COF **34** from a tetrafunctional boronate and 2,2'-bipyridine, and schematic illustration of 2D-network structure. d) Formation of COF **35** from 4-pyridylboronic acid, Monte Carlo simulations of acetylene and CO_2 uptake within porous network structure (bottom), and breakthrough plot for the separation of a $C_2H_2/CO_2/Ar$ (5%/5%/90%) gas mixture at 298 K (right). Adapted with permission from refs. 59 (a), 61b (b), 62 (c), and 63 (d).

^{1}H NMR spectroscopy measurements revealed an entropy-driven disassembly starting at around 320 K with formation of 1:1 and 2:5 complexes, as well as free trisboronate ester (**B3**) (Figure 7b, bottom). The cage was quantitatively regenerated upon cooling to room temperature.

Boroxines also serve as valuable platforms for assembly of molecular cages. In a fascinating early example, Höpfl and coworkers showed that in a single-component self-assembly process 3-pyridylboronic acid forms a pentadecanuclear cage consisting of 5 boroxine units when recrystallized from ethanol.[53] The cage structure was retained in chlorinated solvents as demonstrated by multinuclear NMR experiments and electrospray ionization (ESI) mass spectrometry. In addition, using boroxines as platform molecular cages that undergo shape changes when applying a stimulus have been realized.[54] Iwasawa and coworkers described the pyridine-triggered dynamic transformation of a mixture of 12-mer and 15-mer boroxine cages derived from boronic acid **31** into a 9-mer boroxine cage (Figure 7c).[55] As the geometry of the N-coordinated boron atoms changed from trigonal to tetrahedral, the 9-mer cage became entropically favored.

4. Supramolecular Network Polymers

We have demonstrated that depending on both the number and spatial arrangement of LA/LB functional groups within the building blocks, small molecules self-assemble into 2D macrocycles or 3D cage structures. It is also well established that the repetitive tiling of rigid molecular building units can result in stacked sheet-like 2D structures or interconnected 3D scaffolds.[37, 56] As such, when using building blocks that are capable of forming multiple B-N interactions along certain spatial directions, the formation of (micro)crystalline COFs can be expected. Closely related is the use of molecular building blocks to generate so-called vitrimers, which consist of molecular networks that undergo thermally activated bond-exchange reactions and are of much interest in the search for new robust materials that are amenable to recycling while retaining the desired mechanical properties of typical thermosets.[57] Finally, supramolecular polymer networks[58] in which LP interactions serve as crosslinks between polymer strands are highly attractive in the development of dynamic polymer gels and elastomers.

4.1. Covalent Organic Framework Materials

When connecting a tritopic building block composed of a triboronic acid and 4-tert-butylcatechol with bispyridines as ditopic linkers Severin's group obtained crystalline 2D supramolecular networks (**32**, Figure 8a).[59] Crystallographic analyses revealed B-N bond lengths of 1.676(5) Å (R = none) and 1.678(7) Å (R = vinylene) for **32** similar to those reported for molecular phenylcatecholborane-pyridine adducts. The individual layers were comprised of interwoven large macrocycles, but no catenation between adjacent layers was seen. Thermogravimetric analyses (TGA) and powder X-ray diffraction (PXRD) indicated

that removal of co-crystallized solvent molecules located between layers led to collapse of the crystalline structures. In related work, Höpfl and coworkers utilized self-complementary bifunctional building blocks derived from condensation of pentaerythritol and 4-pyridylboronic acid (or 5-isoquinolineboronic acid) to build up 2D and 3D-network materials through B-N bonding between boronate ester and pyridyl functionalities.[60]

Inspired by these earlier studies, Zhang and coworkers explored the formation of porous framework materials by combining pyridyl-substituted triphenylamine with biphenylene bis(boron catecholate).[61] COF **33** contained 2D sheets that were interlocked and featured micropores with a diameter of ca. 5.5 Å. Consequently, this crystalline framework showed permanent porosity with a Brunauer-Emmett-Teller (BET) surface area of 255 m^2g^{-1}. In contrast to COF **32**, this material exhibited exceptional thermal stability up to 260 °C, proved highly robust toward acids, bases, and even some organic solvents, and could be regenerated by redissolution in hot ethanol/toluene followed by precipitation. More importantly, the authors demonstrated that COF **33** takes up C_2H_2 preferentially over CO_2 gas molecules, allowing for separation of C_2H_2/CO_2 gas mixtures. The preferential uptake of C_2H_2 was rationalized through X-ray analysis of the C_2H_2-loaded COF **33**@C_2H_2 (Figure 8b, inset). π–π interactions of the C_2H_2 molecules with pyridine "panels" and C-H···π interactions with benzene moieties were evident, favoring the selective C_2H_2 gas uptake.

Severin and coworkers also demonstrated that use of a tetrafunctional boronate ester with a tetrahedral core can lead to a 2D network material (**34**, Figure 8c).[62] The defined tetrahedral arrangement of the boronate ester groups meant that the catechol subunits would protrude either above or below the plane of the layer. Throughout the layer the bridging bipyridines were aligned with respect to one another in an alternating fashion, facilitated by rotation of the C-B bonds. However, the intrinsic conformational flexibility of the C-B-N linkage in boronate ester building blocks made it difficult to exert a good level of control over and to predict the geometry of these supramolecular scaffolds.

In pursuit of frameworks with permanent porosity, Hou, Liu and coworkers recently developed a B-N COF (**35**) derived from 4-pyridylboronic acid as a bifunctional monomer.[63] Boroxine condensation resulted in a cyclic trimer to which two pyridines coordinated through dative B-N bonds at a distance of 1.635 Å (Figure 8d). Single crystal analysis showed a *trans*-conformation for the B-coordinated pyridines relative to the boroxine ring. The boroxine nodes further extended into 2D layers which were stacked through weak intermolecular forces. The crystals could be redissolved in hot N-methylformamide and recrystallized by solvent evaporation. PXRD of the as-synthesized and recrystallized samples showed great consistency indicating good solution processability and regenerability enabled by the dynamic B-N interactions. Along the *c*-axis of the framework, channels of 9.0×9.6 Å were seen confirming the porosity of the framework. The guest-free framework produced by extended heating under vacuum exhibited selective gas uptake capability for C_2H_2 / CO_2 mixtures. The selectivity was rationalized through Monte Carlo simulations and a gas adsorption breakthrough experiment with C_2H_2/CO_2 gas mixtures showed longer retention times for C_2H_2 because of stronger hydrogen bonds to the framework (Figure 8d, inset).

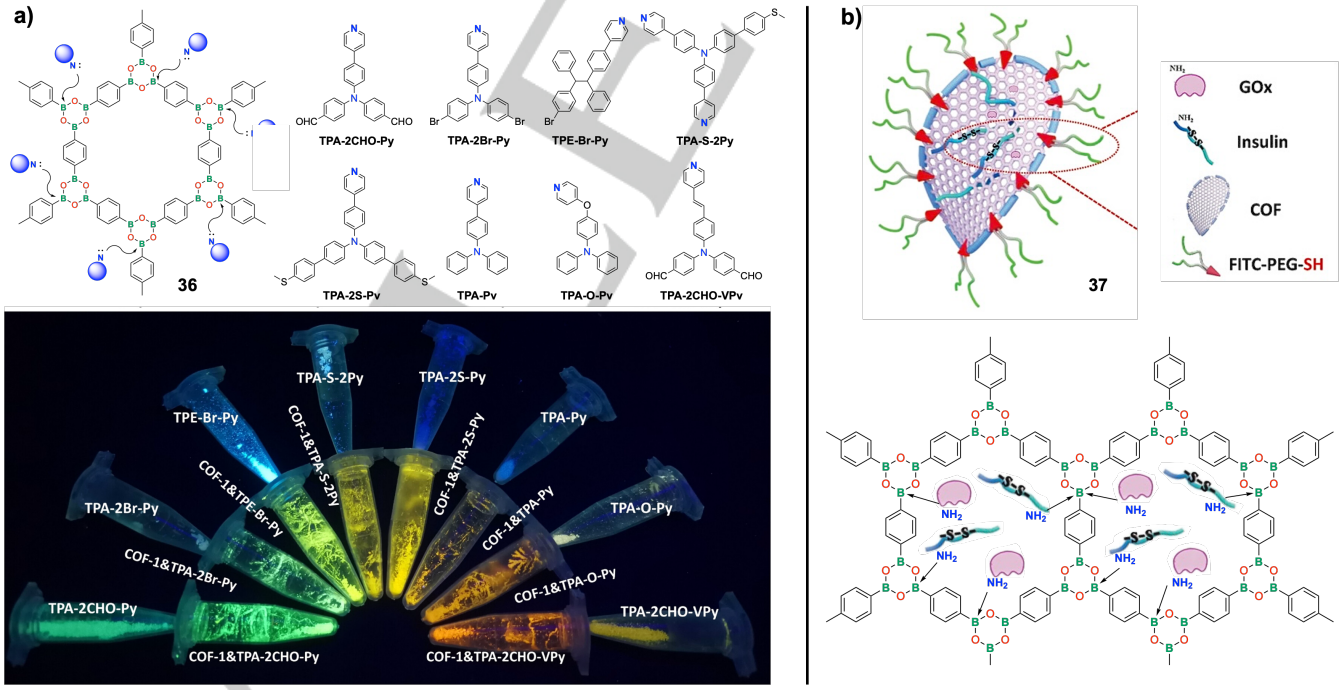

Figure 9. Examples of boroxine-type COFs modified by B-N LP interactions. a) Luminescent materials **36** obtained by binding of pyridyl chromophores to boroxine COFs. b) (top) Schematic illustration of boroxine COF assemblies **37** obtained by binding to amine functionalities of glucose oxidase (GOx) and insulin for drug delivery applications and (bottom) depiction of LP interactions; FITC-PEG-SH = fluorescein isothiocyanate-labeled polyethylene glycol with an SH terminal group. Adapted with permission from ref. 66 (a) and 67 (b).

Recently, the strong binding of pyridines to triarylboranes has been exploited in the development of new robust COF materials with π-conjugated structures.[64] For instance, Ren and coworkers showed that complexes of tris(5-bromothien-2-yl)borane with 4-bromopyridine, 4,4'-bipyridine or 1,3,5-tris(pyridyl)benzene are amenable to Stille coupling polymerization with distannylated thiophene to produce COF materials with B-N LPs as crosslinking points.[65] The products showed interesting low energy ICT absorptions and one of the COFs was studied for photocatalytic H_2 production.

Apart from constructing COFs by B-N LP formation, this interaction can be used to modify the properties of previously established COFs. For example, Ma's group explored the tunable fluorescence of boroxine COFs coordinated with a range of N-donating triphenylamine (TPA) substituted pyridines (**36**, Figure 9a).[66] After incorporating the pyridine dyes on the surface of COF-1, the emission intensities were greatly enhanced. The emission wavelengths were red-shifted relative to the unbound pyridyl-amine dyads because B-N coordination promoted ICT by lowering the electron density on the Py ring. Additionally, the N-coordinated COFs were used to detect 'external' amines as the exchange of the amine Lewis base resulted in fluorescence signal changes.

Dynamic B-N bond formation of COFs with amines was also exploited for biological applications in the field of responsive drug delivery. Jia and coworkers encapsulated amine-containing insulin and glucose oxidase (GOx) within boroxine COFs (COF-1 and COF-5) via a combination of Brønsted acid-base and B-N LP complexation (Figure 9b).[67] Subsequent decoration with fluorescein isothiocyanate-labeled polyethylene glycol (FITC-PEG) through thiol exchange with disulfide bonds in the insulin afforded a stable, fluorescently labeled, water-dispersible polymer-COF nano-assembly (**37**). An increase in acid levels in the presence of glucose, promoted by GOx, was found to result in the decomposition of the boroxine nodes, thus triggering the insulin release. Their work represented the first study on COF-based insulin-delivery nano-carriers for *in vitro* and *in vivo* therapeutic applications.

4.2. Soft Network Polymers with 'Classical' Lewis Pairs

While the materials described above are (micro)crystalline and stand out for their porous nature and ability to take up guest molecules, the use of more flexible linkers between boronic acid moieties can be exploited to develop strong, yet malleable thermosets. Unlike traditional thermoset materials that benefit from favorable mechanical properties but cannot be reprocessed, the dynamic nature of the boroxine ring formation and dative B-N bonding gives rise to fully reprocessable materials. In one example, Guan and coworkers utilized a diboronic acid with a flexible oligoethyleneoxide linker to form boroxine crosslinks in combination with undecylpyridine that not only binds reversibly to the boron atoms but also takes the role of a plasticizer to achieve a highly malleable thermoset.[68] The new thermoset showed a high Young modulus (559 MPa) and tensile strength (17.8 MPa), while also being malleable due to its vitrimer-like properties.

The dynamic nature of B-N LPs has in recent years been further explored for the assembly of stimuli responsive supramolecular polymer networks.[18b] Previous studies demonstrated that the attachment of multiple borane LAs to a polymer could afford interesting properties that enable use as luminescent materials, sensor systems for anions, toxic amines, and other nucleophiles, and as supported catalysts.[69] Our group introduced the first examples of highly Lewis acidic triarylborane-

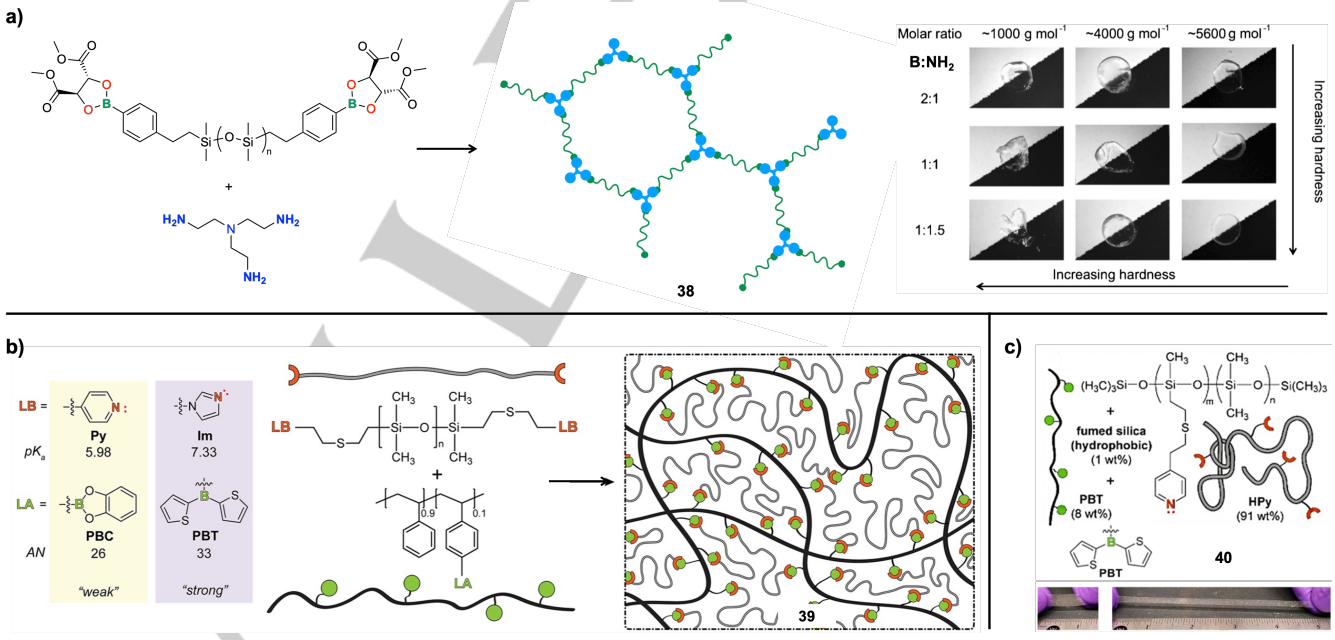

Figure 10. Examples of dynamic polymer networks based on 'classical' B-N LP formation. a) Crosslinking reaction of boronate-terminated poly(dimethylsiloxane) (PDMS) with a trifunctional amine, schematic illustration of the resulting network **38**, and photographs of polymer gels **38** at different B:NH_2 ratios and at different molecular weights of PDMS polymer precursor. b) Formation of polymer gels **39** from polystyrene copolymers with dithienylborane (PBT) and catecholborane (PBC) functional groups in combination with pyridyl (Py) and imidazolyl (Im) terminated PDMS. c) Formation of elastomer **40** by mixing polystyrene copolymers PBT and PDMS containing multiple pyridyl side chains in the presence of 1 wt% fumed silica nanoparticles; bottom: photographs illustrating the (left) pristine and (right) stretched elastomer film of **40**. Adapted with permission from refs. 74 (a) and 75b (b, c).

functionalized polystyrene[70] and demonstrated the anion detection capabilities by changes in the photoluminescence of the boron chromophores when interacting with fluoride or cyanide.[71] More recently, we also investigated the catalytic behavior of polymer-supported electron-deficient triarylboranes in the reductive amination of aldehydes and ketones, and of polymer-supported borinic acids in amide bond formation reactions.[72] When reacting these polymeric LAs with polymer-supported LBs, simultaneous formation of multiple LPs is expected to generate a polymer network with dynamic crosslinks. The crosslinking strength and dynamic properties should be directly correlated with the LP complexation equilibrium,[73] enabling modification of the bulk properties of the resultant polymer networks.[69b]

Brook's group first demonstrated the successful synthesis of thermoplastic silicone elastomers by reversible amine-boronate complex formation, thereby making crosslinked silicones recyclable.[74] A variety of network structures were generated by combining silicones that contain either terminal or pendent boronate groups with tritopic tris(2-aminoethyl)amine (**27**, Figure 10a) or commercially available amino-functionalized silicones (not shown). Various materials ranging from highly crosslinked elastomers to soft polymer gels were obtained, and the increase in crosslinking density afforded stiffer elastomers (Figure 10a, right). Rheological studies showed that at elevated temperatures the viscous modulus overcomes the elastic modulus as the samples effectively melted.

Our group prepared a range of polymer gels by LP formation between polystyrene-supported tricoordinate boranes and terminal pyridyl or imidazolyl groups attached to poly(dimethylsiloxane) (PDMS) (**39**, Figure 10b). The polymer gels exhibited thermo-reversible gel-sol transitions, and experiments on the self-healing capabilities demonstrated the dynamic behavior of the crosslinks.[75] Detailed studies were performed on molecular model systems to examine the equilibrium and dissociation kinetics of the B-N LP crosslinks. Rheological analyses on different gels at variable temperatures suggested a direct correlation between the dissociation kinetics of the B-N LPs and the mechanical properties of the gels, as weaker B-N bonds contributed to lower temperatures for the crossover between the viscous and elastic moduli. Building on these studies, elastomers were prepared by crosslinking polymeric triarylboranes with high molecular weight PDMS containing multiple pendent pyridyl groups (**40**, Figure 10c).[75b] The increased crosslink density and use of strong B-N LPs endowed the polymer networks with enhanced mechanical properties. Tensile tests showed excellent stretchability and improved elasticity of the polymer networks compared to the PDMS precursor. The dative B-N bonds allowed the elastomers to be melt-reprocessed with little to no decrease in the elastic modulus of the reprocessed material compared to the pristine elastomer.

Ding and coworkers combined B-N LPs with H-bonding motifs to construct dually crosslinked polyurethane elastomers with self-healing capabilities at room temperature. N,N-diisopropanolamines and hydroxyl-functionalized phenylene diboronic esters were introduced into the polymer chain at various ratios which led to crosslinked elastomers through the formation of H-bonds and proposed B-N coordination bonds.[8] The authors hypothesized that upon addition of water the boronic esters would hydrolyze to boronic acids, accompanied by dissociation of H-bonds and B-N bonds. Tensile tests of the self-healed elastomers after different time periods demonstrated that the addition of water did accelerate the self-healing efficiency. This phenomenon was more evident for more highly crosslinked polymer networks. However, the self-healed samples did not achieve a comparable mechanical strength to that of the pristine elastomer possibly due to the limited chain movements.

4.3. Soft Network Polymers with 'Frustrated' Lewis Pairs

Besides 'classical' B-N LP interactions, reactions of FLPs and N-containing small molecules with formation of B-N bonds have been exploited for the assembly of crosslinked polymer networks. Studies on the use of molecular FLPs for hydrogenation catalysis and the activation of small molecules (CO, CO_2, N_2O, SO_2, olefins, alkynes, etc) demonstrated the potential of FLPs to promote formation of new dynamic bonds.[4] Furthermore, recently, Stephan and coworkers unequivocally demonstrated that FLPs comprised of $B(C_6H_5)_3$ and PPh_3 react with diethylazodicarboxylate (DEAD) to afford the corresponding diazo-bridged adducts with P-N and N-B linkages whereas more highly Lewis acidic $B(C_6F_5)_3$ and PAr_3 (Ar = Ph, o-Tol, Mes) led to products in which the LPs are linked together via P-N (diazo) and B-O (ester group) bridges.[76]

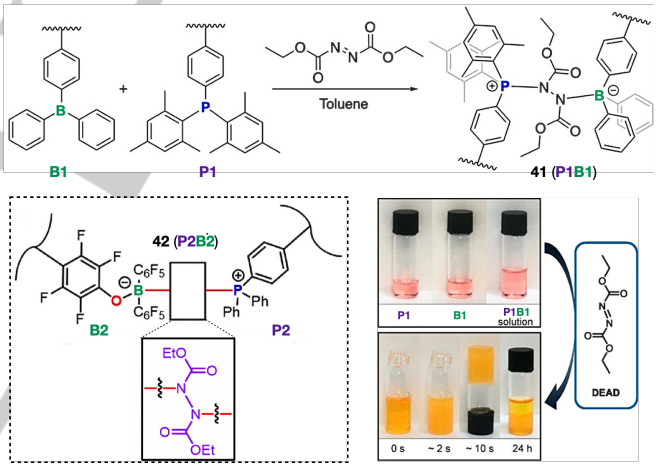

Figure 11. Examples of polymer networks **41** and **42** with dative B-N bonds that are derived from FLP reactions with diethylazodicarboxylate; the photographs illustrate the crosslinking of **P1** and **B1** to form polymer network **30**. Adapted with permission from ref. 77a.

Shaver's group first demonstrated that these chemistries can be applied to construct polystyrene-based crosslinked polymer gels. They prepared a self-healing polymer gel that was derived from RAFT-polymerized polystyrene copolymers with 5 mol% 4-diphenylboryl (**B1**) and 4-dimesitylphosphine (**P1**) functional groups respectively and DEAD as crosslinker (**41**, Figure 11).[77] Upon addition of DEAD (6 equiv.) a homogeneous solution containing non-interacting **B1** and **P1** copolymers in toluene quickly transformed into a gel, accompanied with a color change to orange. With extended reaction time, the dynamic gel rearranged to adopt a thermodynamically more favorable configuration with volume shrinkage. Crosslink formation by coordination of DEAD to the FLPs was also confirmed by IR spectroscopy. Rheology tests showed a crossover between storage (G′) and loss (G″) moduli proving the dynamic nature of the crosslinks. The self-healing ability of the gels was

demonstrated by cutting a brick-shaped gel into two pieces and healing by applying toluene at the interface, as well as by re-solvation of broken xerogels.[77a]

In a continuation of this work, polymers containing 10 mol% bis(pentafluorophenyl)borinic acid tetrafluorophenyl ester groups (**B2**) were synthesized by a two-step post-polymerization modification (Figure 11, inset).[78] An elastic polymer network (**42**, **P2B2**) was then obtained by combining copolymer **B2** with a copolymer containing 4-diphenylphosphine groups (**P2**) and adding DEAD as crosslinker. Rheology experiments showed that across a range of angular frequencies, the G' values were higher than the G" values, confirming the formation of rubber-like networks. The G' values were also higher than those of the previous gel system with its weaker triphenylborane Lewis acid groups. However, the network easily broke down when heated and was susceptible to degradation in air, suggesting that some defects were generated during gelation. Collectively, these results demonstrated that FLP reactions with azo compounds accompanied by the formation of dynamic B-N bonds can serve as a powerful tool for the formation of self-healing and recyclable polymer networks.

We note that this chemistry is not restricted to the activation of diazo species with formation of dative B-N bonds but has also been successfully applied by Yan and coworkers to CO_2 activation with concomitant formation of crosslinked polymeric materials with P-C and B-O linkages.[79] Micellar systems were generated by employing random-block copolymers that comprised an unfunctionalized polystyrene block and a borane- or phosphine-functionalized block respectively,[79a] whereas assembly of copolymers containing both borane and phosphine functional groups resulted in single-chain polymer nanoparticles.[79b] Furthermore, Shaver and coworkers have recently reported the crosslinking of B- and P-functionalized FLP-type polymers with epoxides, as well as with a mixture of CO_2 and epoxides.[80]

5. Conclusions and Outlook

We have demonstrated how B-N LP formation, while long established in small molecule chemistries and extensively utilized in molecular recognition, small molecule activation, and to tune the (opto)electronic properties of conjugated materials, has recently emerged as a powerful tool for assembly of functional supramolecular oligomeric and polymeric materials. Combinations of bifunctional building blocks that contain two LA groups with bifunctional building blocks that contain two LB groups have been exploited to generate dynamic macrocycles and linear polymers, including systems with interesting CT, emissive, and redox-responsive properties. When using building blocks that contain three or more functional groups, molecular cages that serve as hosts for small molecules, COFs that take up and separate gases and are utilized in sensors and biomedical applications, and supramolecular polymer networks in the form of vitrimers, gels, and elastomers, are obtained. All these materials have in common that the tunable dative B-N bonds enable their assembly and disassembly on demand, an aspect that allows for stimuli-responsiveness, dynamic molecular shape changes, and is particularly important in the development of new 3-D materials that are notoriously difficult to recycle and reuse when 'traditional' covalent bonding is employed in their construction.

While this review has been focused on materials with dative B-N bonds, other Lewis acid-base interactions can be employed, including those involving the heavier Group 13 elements[81] or the heavier elements from Group 14-17 that are capable of hypervalent[82] bonding. Similarly, Lewis basic building blocks that contain other Group 15 and Group 16 elements are highly promising. Systems with P that involve FLP-type chemistries have already received much attention and, for example, oxygen-based quinone systems show exciting properties such as dynamic radical formation when combined with borane Lewis acids.[83] This leaves much room for new innovations and the development of functional materials with exciting and unprecedented properties.

Acknowledgements

This review was assembled with support by the National Science Foundation under Grant No. [1904791]. Supplement funding for this project was provided by the Rutgers University – Newark Chancellor's Research Office. F. J. is grateful to all his current and former coworkers and collaborators who contributed to the research discussed in here.

Keywords: boron • Lewis pairs • macrocycles • polymers • supramolecular materials

[1] G. N. Lewis, *Valence and the Structure of Atoms and Molecules*, Chemical Catalogue Company, New York, **1923**.

[2] H. C. Brown, H. I. Schlesinger, S. Z. Cardon, *J. Am. Chem. Soc.* **1942**, *64*, 325-329.

[3] G. C. Welch, R. R. San Juan, J. D. Masuda, D. W. Stephan, *Science* **2006**, *314*, 1124-1126.

[4] D. W. Stephan, *Science* **2016**, *354*, aaf7229.

[5] A. Staubitz, A. P. M. Robertson, M. E. Sloan, I. Manners, *Chem. Rev.* **2010**, *110*, 4023-4078.

[6] C. R. Wade, A. E. J. Broomsgrove, S. Aldridge, F. P. Gabbai, *Chem. Rev.* **2010**, *110*, 3958-3984.

[7] H. E. Katz, *J. Org. Chem.* **1985**, *50*, 5027-5032.

[8] a) F. Jäkle, T. Priermeier, M. Wagner, *Chem. Commun.* **1995**, 1765-1766; b) E. Herdtweck, F. Jäkle, M. Wagner, *Organometallics* **1997**, *16*, 4737-4745; c) J. F. Chai, S. P. Lewis, S. Collins, T. J. J. Sciarone, L. D. Henderson, P. A. Chase, G. J. Irvine, W. E. Piers, M. R. J. Elsegood, W. Clegg, *Organometallics* **2007**, *26*, 5667-5679; d) A. Lorbach, M. Bolte, H. W. Lerner, M. Wagner, *Chem. Commun.* **2010**, *46*, 3592-3594; e) C. H. Chen, F. P. Gabbai, *Chem. Sci.* **2018**, *9*, 6210-6218; f) P. Niermeier, S. Blomeyer, Y. K. J. Bejaoui, J. L. Beckmann, B. Neumann, H. G. Stammler, N. W. Mitzel, *Angew. Chem. Int. Ed.* **2019**, *58*, 1965-1969; g) A. Widera, H. Wadepohl, H.-J. Himmel, *Angew. Chem. Int. Ed.* **2019**, *58*, 5897-5901.

[9] a) B. L. Wang, Y. X. Li, R. Ganguly, H. Hirao, R. Kinjo, *Nat. Commun.* **2016**, *7*, 11871; b) J. J. Kiernicki, M. Zeller, N. K. Szymczak, *J. Am. Chem. Soc.* **2017**, *139*, 18194-18197; c) J. W. Taylor, A. McSkimming, C. F. Guzman, W. H. Harman, *J. Am. Chem. Soc.* **2017**, *139*, 11032-11035; d) S. Xu, L. A. Essex, J. Q. Nguyen, P. Farias, J. W. Ziller, W. H. Harman, W. J. Evans, *Dalton Trans.* **2021**, *50*, 15000-15002; e) D. M. Beagan, J. J. Kiernicki, M. Zeller, N. K. Szymczak, *Angew. Chem. Int. Ed.* **2023**, *62*, e202218907; f) S. N. Kessler, H. A. Wegner, *Org. Lett.* **2010**, *12*, 4062-4065; g) L. Schweighauser, H. A. Wegner, *Chem. Eur. J.* **2016**, *22*, 14094-14103.

[10] a) G. Campillo-Alvarado, K. P. D'mello, D. C. Swenson, S. V. S. Mariappan, H. Höpfl, H. Morales-Rojas, L. R. MacGillivray, *Angew. Chem. Int. Ed.* **2019**, *58*, 5413-5416;

b) S. Bhandary, M. Belis, A. M. Kaczmarek, K. Van Hecke, *J. Am. Chem. Soc.* **2022**, *144*, 22051–22058.

[11] S. Bhandary, M. Belis, L. Bourda, A. M. Kaczmarek, K. Van Hecke, *Angew. Chem. Int. Ed.* **2023**, *62*, e202304722.

[12] G. C. Welch, G. C. Bazan, *J. Am. Chem. Soc.* **2011**, *133*, 4632-4644.

[13] a) T. Ono, M. Sugimoto, Y. Hisaeda, *J. Am. Chem. Soc.* **2015**, *137*, 9519-9522; b) Y. Yano, H. Kasai, Y. Y. Zheng, E. Nishibori, Y. Hisaeda, T. Ono, *Angew. Chem. Int. Ed.* **2022**, *61*, e202203853; c) J. Zou, Y. Fang, Y. Shen, Y. Xia, K. Wang, C. Zhang, Y. Zhang *Angew. Chem. Int. Ed.* **2022**, *61*, e202207426.

[14] a) I. A. Boenig, W. R. Conway, K. Niedenzu, *Synth. React. Inorg. Met.-Org. Chem.* **1975**, *5*, 1-5; b) K. D. Müller, L. Komorowski, K. Niedenzu, *Synth. React. Inorg. Met. Chem.* **1978**, *8*, 149-155.

[15] C. P. Brock, A. L. Companion, L. D. Kock, K. Niedenzu, *Inorg Chem* **1991**, *30*, 784-789.

[16] a) N. Fujita, S. Shinkai, T. D. James, *Chem. Asian J.* **2008**, *3*, 1076-1091; b) R. Nishiyabu, Y. Kubo, T. D. James, J. S. Fossey, *Chem. Commun.* **2011**, *47*, 1124-1150.

[17] A. L. Korich, P. M. Iovine, *Dalton Trans.* **2010**, *39*, 1423-1431.

[18] a) C. Z. He, J. Dong, C. R. Xu, X. C. Pan, *ACS Polym. Au* **2023**, *3*, 5-27; b) Z. H. Zhao, C. H. Li, J. L. Zuo, *SmartMat* **2023**, *4*, e1187.

[19] a) F. Jäkle, *Chem. Rev.* **2010**, *110*, 3985-4022; b) K. Tanaka, Y. Chujo, *Macromol. Rapid Comm.* **2012**, *33*, 1235-1255; c) F. Jäkle, *Top. Organomet. Chem. (Springer)* **2015**, *49*, 297-325; d) H. Helten, *Chem.-Eur. J.* **2016**, *22*, 12972-12982; e) Y. Ren, F. Jäkle, in *Main Group Strategies towards Functional Hybrid Materials* (Eds.: T. Baumgartner, F. Jäkle), John Wiley and Sons, Chichester, **2018**, pp. 79-110.

[20] a) L. Brunsveld, B. J. B. Folmer, E. W. Meijer, R. P. Sijbesma, *Chem. Rev.* **2001**, *101*, 4071-4098; b) L. L. Yang, X. X. Tan, Z. Q. Wang, X. Zhang, *Chem. Rev.* **2015**, *115*, 7196-7239; c) S. Samanta, S. Kim, T. Saito, A. P. Sokolov, *J. Phys. Chem. B* **2021**, *125*, 9389-9401; d) D. Shimoyama, F. Jäkle, *Aggregate* **2022**, *3*, e149.

[21] a) K. Severin, *Dalton Trans.* **2009**, 5254-5264; b) M. Nakahata, S. Sakai, *Chemnanomat* **2019**, *5*, 141-151; c) M. M. Perera, N. Ayres, *Polym. Chem.* **2020**, *11*, 1410-1423; d) A. P. Bapat, B. S. Sumerlin, A. Sutti, *Mater. Horiz.* **2020**, *7*, 694-714; e) M. Gosecki, M. Gosecka, *Polymers* **2022**, *14*, 842.

[22] N. Christinat, E. Croisier, R. Scopelliti, M. Cascella, U. Röthlisberger, K. Severin, *Eur. J. Inorg. Chem.* **2007**, 5177-5181.

[23] D. Salazar-Mendoza, J. Cruz-Huerta, H. Höpfl, I. F. Hernandez-Ahuactzi, M. Sanchez, *Cryst. Growth Des.* **2013**, *13*, 2441-2454.

[24] E. Sheepwash, N. Luisier, M. R. Krause, S. Noé, S. Kubik, K. Severin, *Chem. Commun.* **2012**, *48*, 7808-7810.

[25] N. Luisier, R. Scopelliti, K. Severin, *Soft Matter* **2016**, *12*, 588-593.

[26] J. Cruz-Huerta, G. Campillo-Alvarado, H. Höpfl, P. Rodriguez-Cuamatzi, V. Reyes-Marquez, J. Guerrero-Alvarez, D. Salazar-Mendoza, N. Farfan-Garcia, *Eur. J. Inorg. Chem.* **2016**, 355-365.

[27] A. Torres-Huerta, M. D. Velasquez-Hernandez, D. Martinez-Otero, H. Höpfl, V. Jancik, *Cryst. Growth Des.* **2017**, *17*, 2438-2452.

[28] S. Bhandary, R. Shukla, K. Van Hecke, *Crystengcomm* **2022**, *24*, 1695-1699.

[29] M. Fontani, F. Peters, W. Scherer, W. Wachter, M. Wagner, P. Zanello, *Eur. J. Inorg. Chem.* **1998**, 1453-1465.

[30] M. Grosche, E. Herdtweck, F. Peters, M. Wagner, *Organometallics* **1999**, *18*, 4669-4672.

[31] N. Matsumi, A. Kagata, K. Aoi, *J. Power Sources* **2010**, *195*, 6182-6186.

[32] Y. Qin, C. Cui, F. Jäkle, *Macromolecules* **2007**, *40*, 1413-1420.

[33] A. Staubitz, A. P. M. Robertson, I. Manners, *Chem. Rev.* **2010**, *110*, 4079-4124.

[34] A. Ledoux, P. Larini, C. Boisson, V. Monteil, J. Raynaud, E. Lacote, *Angew. Chem. Int. Ed.* **2015**, *54*, 15744-15749.

[35] a) H. Dorn, R. A. Singh, J. A. Massey, J. M. Nelson, C. A. Jaska, A. J. Lough, I. Manners, *J. Am. Chem. Soc.* **2000**, *122*, 6669-6678; b) H. C. Johnson, E. M. Leitao, G. R. Whitten, I. Manners, G. C. Lloyd-Jones, A. S. Weller, *J. Am. Chem. Soc.* **2014**, *136*, 9078-9093.

[36] B. Adelizzi, P. Chidchob, N. Tanaka, B. A. G. Lamers, S. C. J. Meskers, S. Ogi, A. R. A. Palmans, S. Yamaguchi, E. W. Meijer, *J. Am. Chem. Soc.* **2020**, *142*, 16681-16689.

[37] F. Beuerle, B. Gole, *Angew. Chem. Int. Ed.* **2018**, *57*, 4850-4878.

[38] a) P. K. Chen, F. Jäkle, *J. Am. Chem. Soc.* **2011**, *133*, 20142-20145; b) F. P. Gabbai, *Angew. Chem. Int. Ed.* **2012**, *51*, 6316-6318; c) D. Shimoyama, N. Baser-Kirazli, R. A. Lalancette, F. Jäkle, *Angew. Chem. Int. Ed.* **2021**, *60*, 17942-17946; d) Y. H. Wu, S. C. Li, H. K. Li, R. Q. Ye, Z. P. Lu, *J. Mater. Chem. C* **2023**, *11*, 7144-7158; e) J. F. Chen, Q. X. Gao, L. J. Liu, P. K. Chen, T. B. Wei, *Chem. Sci.* **2023**, *14*, 987-993.

[39] A. Weiss, H. Pritzkow, W. Siebert, *Angew. Chem. Int. Ed.* **2000**, *39*, 547-549.

[40] N. Christinat, R. Scopelliti, K. Severin, *J. Org. Chem.* **2007**, *72*, 2192-2200.

[41] Y. Sugihara, K. Takakura, T. Murafuji, R. Miyatake, K. Nakasuji, M. Kato, S. Yano, *J. Org. Chem.* **1996**, *61*, 6829-6834.

[42] S. Wakabayashi, M. Kuse, A. Kida, S. Komeda, K. Tatsumi, Y. Sugihara, *Org. Biomol. Chem.* **2014**, *12*, 5382-5387.

[43] S. Wakabayashi, Y. Sugihara, K. Takakura, S. Murata, H. Tomioka, S. Ohnishi, K. Tatsumi, *J. Org. Chem.* **1999**, *64*, 6999-7008.

[44] S. Wakabayashi, Y. Hori, S. Komeda, Y. Shimizu, Y. Ohki, M. Horiuchi, T. Itoh, Y. Sugihara, K. Tatsumi, *J. Org. Chem.* **2016**, *81*, 2399-2404.

[45] S. Wakabayashi, N. Sugiyama, Y. Ohki, T. Itoh, T. Kitagawa, *Chem. Asian J.* **2019**, *14*, 568-573.

[46] S. Wakabayashi, M. Takumi, S. Kamio, M. Wakioka, Y. Ohki, A. Nagaki, *Chem. Eur. J.* **2022**, *29*, e202202882.

[47] J. He, F. Rauch, A. Friedrich, J. Krebs, I. Krummenacher, R. Bertermann, J. Nitsch, H. Braunschweig, M. Finze, T. B. Marder, *Angew. Chem. Int. Ed.* **2021**, *60*, 4833-4840.

[48] L. Ding, K. B. Ma, G. Durner, M. Bolte, F. F. de Biani, P. Zanello, M. Wagner, *J. Chem. Soc., Dalton Trans.* **2002**, 1566-1573.

[49] A. Widera, E. Filbeck, H. Wadepohl, E. Kaifer, H. J. Himmel, *Chem. Eur. J.* **2020**, *26*, 3435-3440.

[50] E. Filbeck, A. Widera, E. Kaifer, H. J. Himmel, *Chem. Eur. J.* **2021**, *27*, 15737-15750.

[51] B. Icli, E. Sheepwash, T. Riis-Johannessen, K. Schenk, Y. Filinchuk, R. Scopelliti, K. Severin, *Chem. Sci.* **2011**, *2*, 1719-1721.

[52] A. Dhara, F. Beuerle, *Chem. Eur. J.* **2015**, *21*, 17391-17396.

[53] N. Farfán, H. Höpfl, V. Barba, M. E. Ochoa, R. Santillan, E. Gómez, A. Gutiérrez, *J. Organomet. Chem.* **1999**, *581*, 70-81.

[54] K. Ono, N. Iwasawa, *Chem. Eur. J.* **2018**, *24*, 17856-17868.

[55] K. Ono, S. Shimo, K. Takahashi, N. Yasuda, H. Uekusa, N. Iwasawa, *Angew. Chem. Int. Ed.* **2018**, *57*, 3113-3117.

[56] K. Y. Geng, T. He, R. Y. Liu, S. Dalapati, K. T. Tan, Z. P. Li, S. S. Tao, Y. F. Gong, Q. H. Jiang, D. L. Jiang, *Chem. Rev.* **2020**, *120*, 8814-8933.

[57] N. J. Van Zee, R. Nicolay, *Prog. Polym. Sci.* **2020**, *104*, 101233.

[58] A. M. Wemyss, C. Ellingford, Y. Morishita, C. Bowen, C. Y. Wan, *Angew. Chem. Int. Ed.* **2021**, *60*, 13725-13736.

[59] E. Sheepwash, V. Krampl, R. Scopelliti, O. Sereda, A. Neels, K. Severin, *Angew. Chem. Int. Ed.* **2011**, *50*, 3034-3037.
[60] J. Cruz-Huerta, D. Salazar-Mendoza, J. Hernandez-Paredes, I. F. H. Ahuactzi, H. Höpfl, *Chem. Commun.* **2012**, *48*, 4241-4243.
[61] a) F. Y. Li, X. Xiao, Q. Xu, *Chem* **2023**, *9*, 13-15; b) H. Zhang, Y. B. Li, L. J. Chen, Y. S. Yang, H. Y. Lin, S. C. Xiang, B. L. Chen, Z. J. Zhang, *Chem* **2023**, *9*, 242-252.
[62] A. J. Stephens, R. Scopelliti, F. F. Tirani, E. Solari, K. Severin, *Acs Mater. Lett.* **2019**, *1*, 3-7.
[63] W. Wang, L. Wang, F. Du, G. D. Wang, L. Hou, Z. Zhu, B. Liu, Y. Y. Wang, *Chem. Sci.* **2023**, *14*, 533-539.
[64] F. Qiu, W. X. Zhao, S. Han, X. D. Zhuang, H. L. Lin, F. Zhang, *Polymers* **2016**, *8*, 191.
[65] X. Han, C. Xue, Z. Zhao, M. Peng, Q. Wang, H. Liu, N. Yu, C. Pu, Y. Ren, *ACS Macro Lett.* **2023**, *12*, 961-967.
[66] Y. Sun, B. Zhang, C. Zhang, H. Lu, Y. Yang, B. Han, F. Dong, J. Lv, S. Zhang, Z. Li, Z. Lei, H. Ma, *ACS Appl. Mater. Interf.* **2023**, *15*, 4569-4579.
[67] G. Y. Zhang, Y. Ji, X. L. Li, X. Y. Wang, M. M. Song, H. L. Gou, S. Gao, X. D. Jia, *Adv. Healthc. Mater.* **2020**, *9*, 2000221.
[68] W. A. Ogden, Z. Guan, *J. Am. Chem. Soc.* **2018**, *140*, 6217-6220.
[69] a) F. Jäkle, *Coord. Chem. Rev.* **2006**, *250*, 1107-1121; b) U. Yolsal, T. A. R. Horton, M. Wang, M. P. Shaver, *Progr. Polym. Sci.* **2020**, *111*, 101313.
[70] Y. Qin, G. Cheng, A. Sundararaman, F. Jäkle, *J. Am. Chem. Soc.* **2002**, *124*, 12672-12673.
[71] a) K. Parab, K. Venkatasubbaiah, F. Jäkle, *J. Am. Chem. Soc.* **2006**, *128*, 12879-12885; b) F. Cheng, E. M. Bonder, F. Jäkle, *J. Am. Chem. Soc.* **2013**, *135*, 17286-17289.
[72] a) M. K. Baraniak, R. A. Lalancette, F. Jäkle, *Chem. Eur. J.* **2019**, *25*, 13799-13810; b) F. Vidal, J. McQuade, R. Lalancette, F. Jäkle, *J. Am. Chem. Soc.* **2020**, *142*, 14427-14431.
[73] Y. Qin, F. Jäkle, *J. Inorg. Organomet. Polym. Mater.* **2007**, *17*, 149-157.
[74] L. Dodge, Y. Chen, M. A. Brook, *Chem. Eur. J.* **2014**, *20*, 9349-9356.
[75] a) F. Vidal, H. Lin, C. Morales, F. Jäkle, *Molecules* **2018**, *23*, 405; b) F. Vidal, J. Gomezcoello, R. A. Lalancette, F. Jäkle, *J. Am. Chem. Soc.* **2019**, *141*, 15963-15971.
[76] D. Mandal, T. Chen, Z.-W. Qu, S. Grimme, D. W. Stephan, *Chem. Eur. J.* **2022**, *28*, e202201701.
[77] a) M. Wang, F. Nudelman, R. R. Matthes, M. P. Shaver, *J. Am. Chem. Soc.* **2017**, *139*, 14232-14236; b) U. Yolsal, M. Wang, J. R. Royer, M. P. Shaver, *Macromolecules* **2019**, *52*, 3417-3425.
[78] M. Wang, J. Holland, T. A. R. Horton, U. Yolsal, M. P. Shaver, *Polymer* **2022**, *242*, 124576.
[79] a) L. Chen, R. Liu, Q. Yan, *Angew. Chem. Int. Ed.* **2018**, *57*, 9336-9340; b) R. Zeng, L. Chen, Q. Yan, *Angew. Chem. Int. Ed.* **2020**, *59*, 18418-18422; c) R. Liu, Y. Wang, Q. Yan, *Macromol. Rapid Comm.* **2021**, *42*, 2000699.
[80] a) U. Yolsal, T. A. R. Horton, M. Wang, M. P. Shaver, *J. Am. Chem. Soc.* **2021**, *143*, 12980-12984; b) T. A. R. Horton, M. Wang, M. P. Shaver, *Chem. Sci.* **2022**, *13*, 3845-3850.
[81] a) P. Jutzi, N. Lenze, B. Neumann, H.-G. Stammler, *Angew. Chem. Int. Ed.* **2001**, *40*, 1423-1427; b) J. Horstmann, M. Hyseni, A. Mix, B. Neumann, H. G. Stammler, N. W. Mitzel, *Angew. Chem. Int. Ed.* **2017**, *56*, 6107-6111; c) N. W. Mitzel, N. Aders, P. C. Trapp, J. H. Lamm, J. L. Beckmann, B. Neumann, H. G. Stammler, *Organometallics* **2022**, *41*, 3600-3611.
[82] J. I. Musher, *Angew. Chem. Int. Ed.* **1969**, *8*, 54-68.
[83] X. Dong, Q.-C. Luo, Y. Zhao, T. Wang, Q. Sun, R. Pei, Y. Zhao, Y.-Z. Zheng, X. Wang, *J. Am. Chem. Soc.* **2023**, *145*, 17292-17298.